

## Supporting Information for

# Are Sodiation/De-Sodiation Reactions Reversible in Two-Dimensional Metallic NbSe<sub>2</sub>?

Zaichun Liu, Rui Wang, Panpan Zhang, Chaochao Dun, Jeffrey J. Urban, Sheng Yang, Tao Wang, Yuan Ma, Yiren Zhong, Jiarui He, Zhi Zhu, Xiaosong Xiong, Weijia Fan, Qi Zhou, Haoyuan Yang, Xin-Bing Cheng, Faxing Wang\*, Ying Huang\*, and Yuping Wu\*

\*Corresponding authors: F. Wang, Y. Huang, and Y. Wu

E-mail: wuyp@seu.edu.cn (Y.W.), yinghuang215@hotmail.com (Y.H.), faxing.wang@seu.edu.cn (F.W.)

This PDF file includes:

Figs. S1 to S9

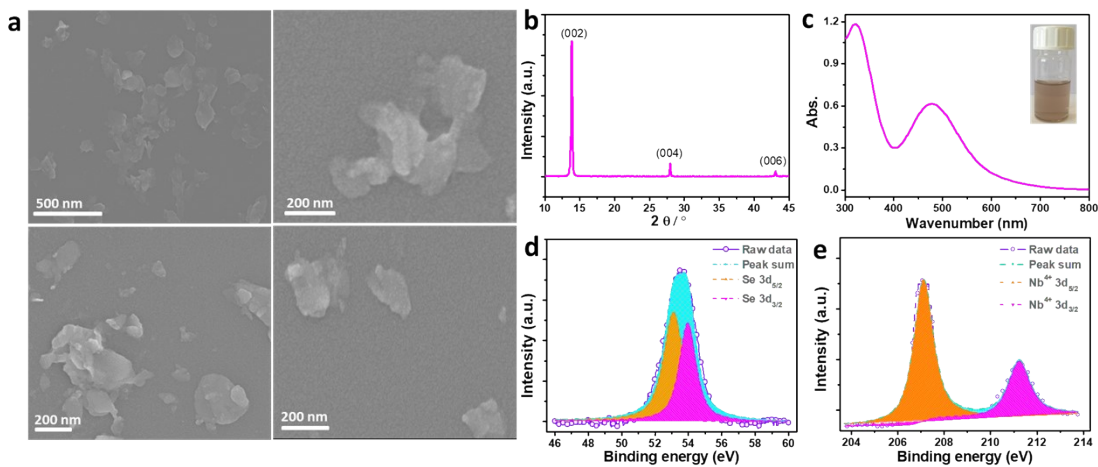


**Fig. S1** (a) SEM images of exfoliated  $\text{NbSe}_2$  samples with different magnifications. (b) XRD pattern of exfoliated  $\text{NbSe}_2$  samples. (c) UV absorbance spectrum of exfoliated  $\text{NbSe}_2$  samples. The insert is a photograph of typically  $\text{NbSe}_2$  flake dispersion. XPS spectra of (d) Se 3d and (e) Nb 3d peaks from  $\text{NbSe}_2$  flakes. The Se species can be fitted with Se  $3\text{d}_{5/2}$  (53.2 eV) and Se  $3\text{d}_{3/2}$  (54.1 eV) peaks in agreement with the  $\text{Se}^{2+}$  state. The two peaks at 203.0 and 206.5 eV correspond to the  $\text{Nb}^{4+}$  state.

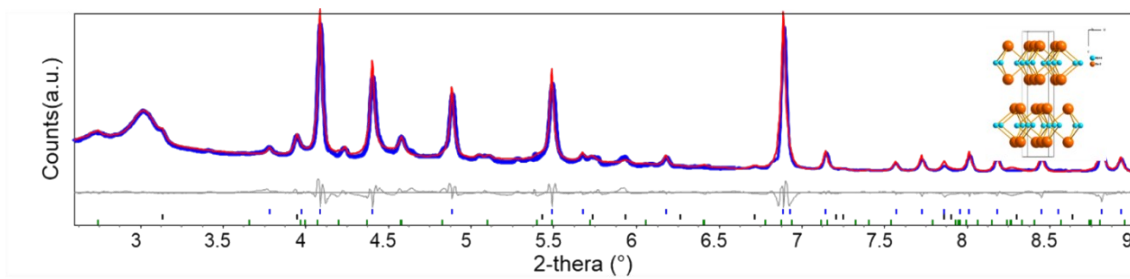


**Fig. S2** Synchrotron XRD patterns of NbSe<sub>2</sub> flakes and Rietveld analysis.

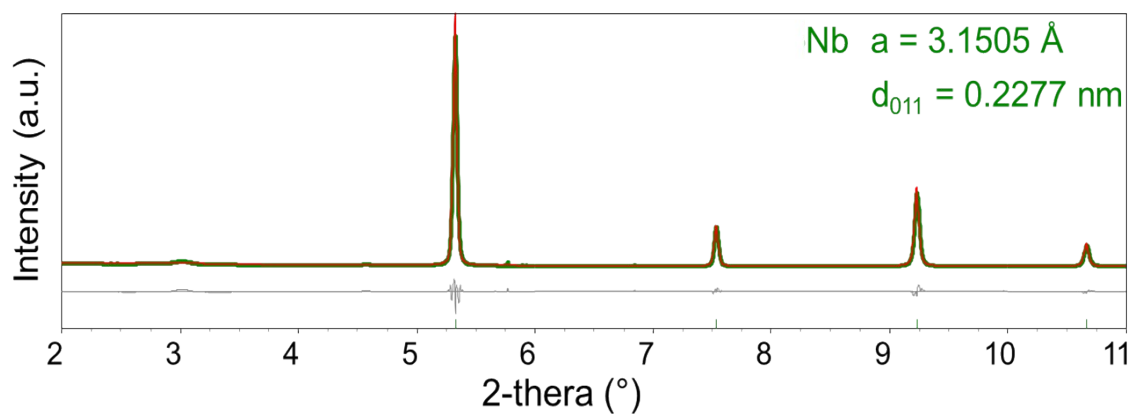


**Fig. S3** Synchrotron XRD patterns of Nb metal reference and Rietveld analysis.

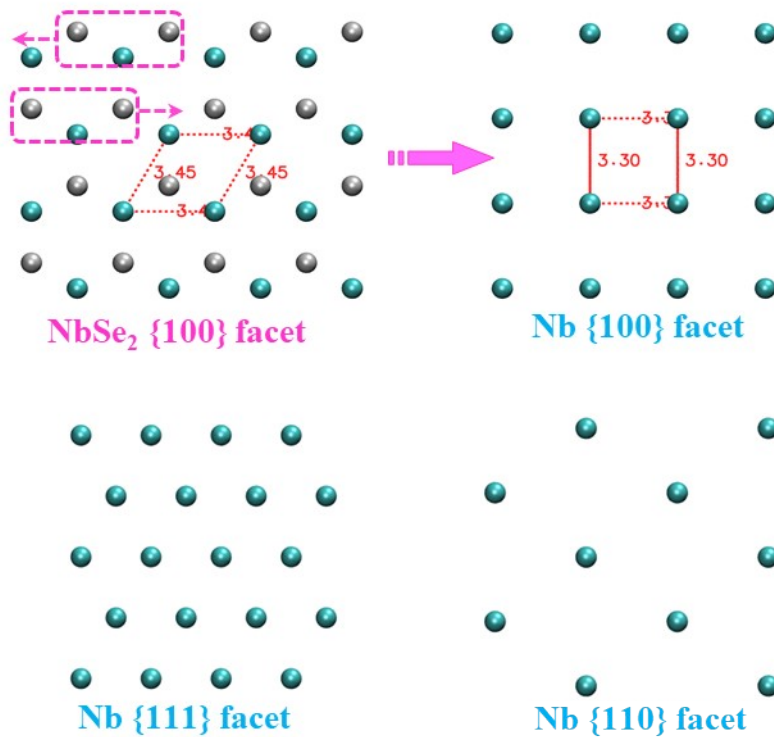


**Fig. S4** Schematic illustration of the topotactic conversion reaction and lattice models of Nb atoms in the crystal structures of  $\text{NbSe}_2$  ( $4 \times 4$  supercells with 48 atoms) and bcc Nb ( $4 \times 4$  supercells with 16 atoms in the surface layer). The grey and blue spheres represent Se and Nb atoms, respectively.

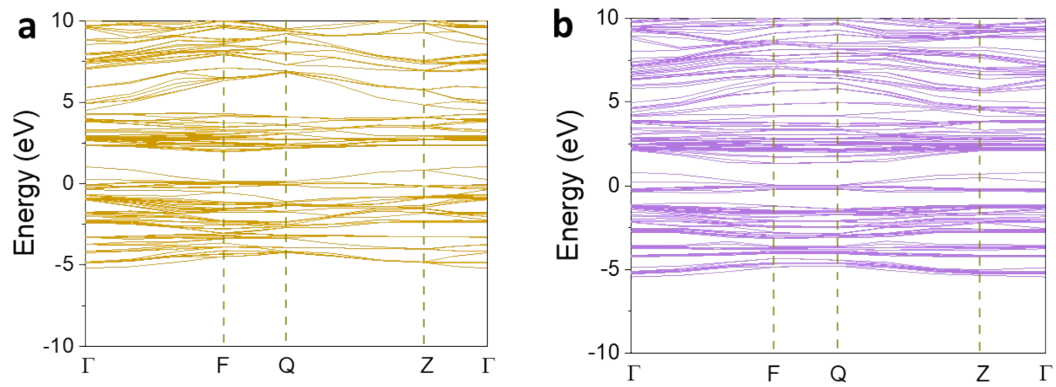


**Fig. S5** Band structures of (a)  $\text{NbSe}_2$  and (b)  $\text{Na}_x\text{NbSe}_2$ .

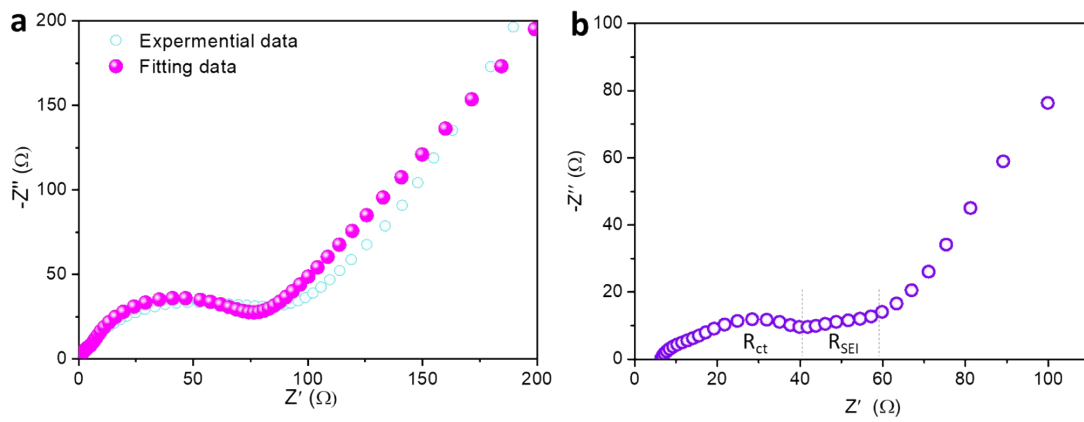


**Fig. S6** Electrochemical impedance spectroscopy (EIS) of (a) pristine  $\text{NbSe}_2$  electrodes and (b)  $\text{NbSe}_2$  electrode after 240 cycles.

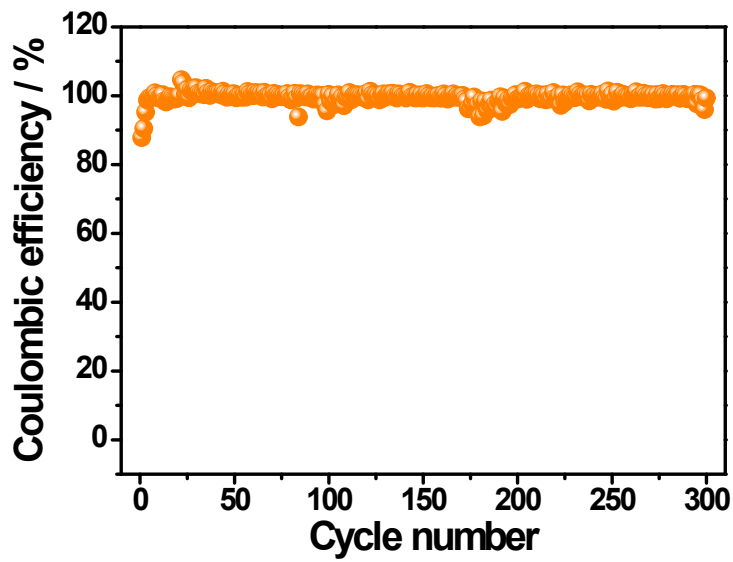


**Fig. S7** The Coulombic efficiency of the assembled dual-ion battery based on activated NbSe<sub>2</sub> anode and graphite cathode.

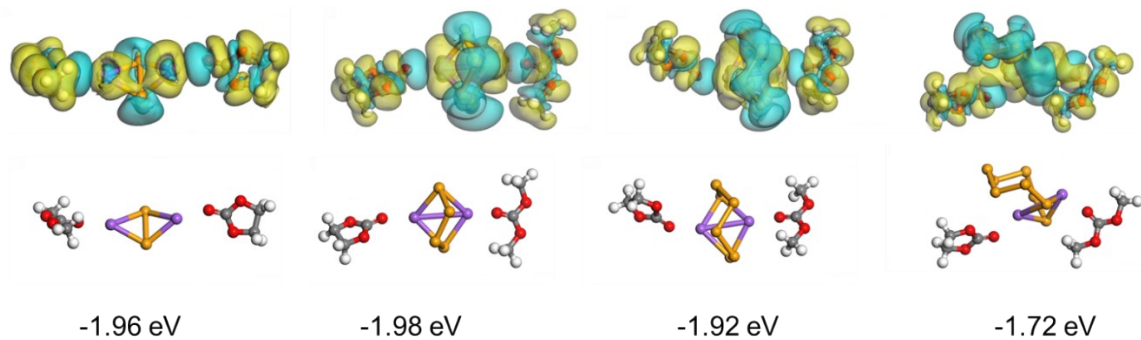


**Fig. S8** The calculated dissolution energy of intermediate  $\text{Na}_2\text{Se}_x$  species in the used electrolyte solvents.

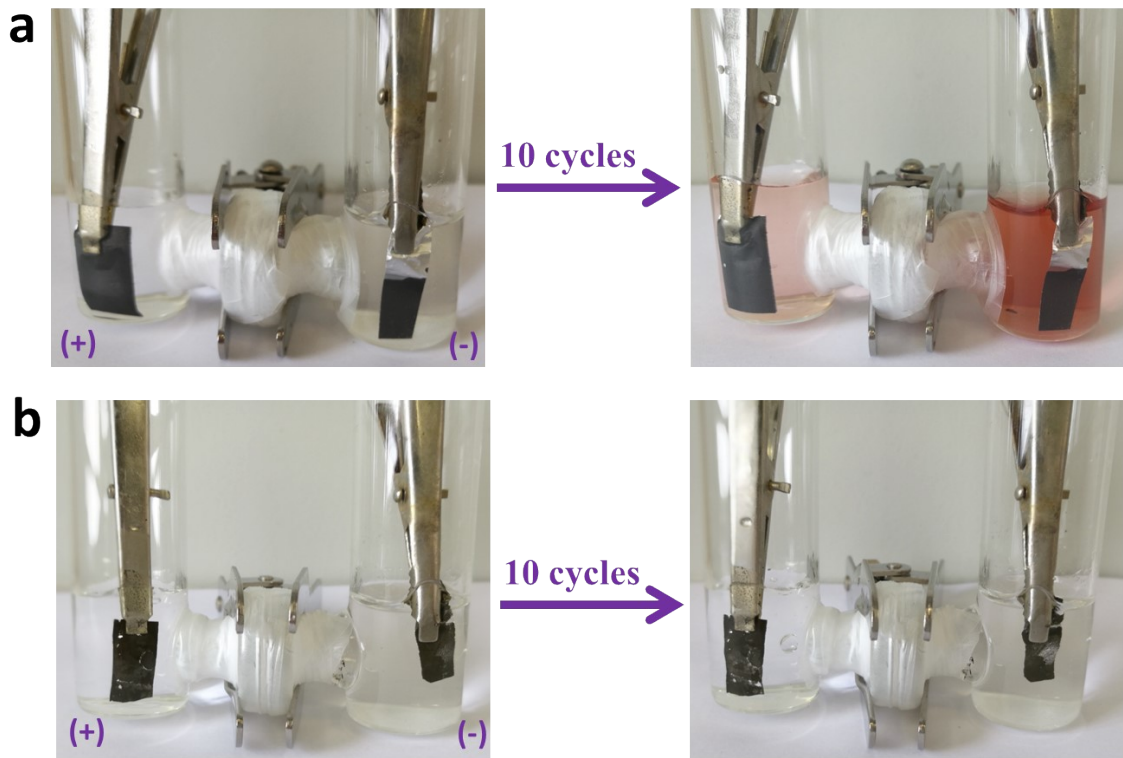


**Fig. S9** Photographs of the dual-ion battery using (a) pure Se and (b) Nb/Se (activated NbSe<sub>2</sub>) anodes in a two-electrode glass cell device. To understand the inhibition effect of polyselenides, two-electrode glass battery device was assembled to observe the dissolution behavior during charge/discharge process.

**Table S1.** Main electrochemical performance parameters of NbSe<sub>2</sub> based electrodes in half-cell tests.

Electrodes	Stored metal ion	Maximum reversible capacity / mAh g <sup>-1</sup>	Cycle/capacity retention	Ref.
NbSe <sub>2</sub> nanosheets	Li-ion	347	-	1
NbSe <sub>2</sub> nanoparticles	Li-ion	313	-	2
	Mg-ion	101	42% after 40 cycles	
NbSe <sub>2</sub> flakes	K-ion	115	91% after 40 cycles	3
NbSe <sub>2</sub> flakes	Na-ion	~125	84% after 100 cycles	4
NbSe <sub>2</sub> nanoparticles	Na-ion	154	94% after 100 cycles	5
	Li-ion	485	83% after 100 cycles	
NbSe <sub>2</sub> / N,Se co-doped CNFs	K-ion	288	~100% after 1200 cycles	6
NbSe <sub>2</sub> @graphene	Li-ion	489	>100% after 1000 cycles	7
Flower-like Nb <sub>2</sub> Se <sub>9</sub>	Li-ion	672	88% after 250 cycles	8
	Na-ion	342	52% after 250 cycles	
NbSe <sub>2</sub> /SnSe	K-ion	~375	~75% after 1000 cycles	9
NbSe <sub>2</sub> /NbS <sub>2</sub>	Na-ion	~200	92% after 500 cycles	10
NbSe <sub>2</sub> flakes	Na-ion	212	72% after 500 cycles	This work

## References

1. E. Hitz, J. Wan, A. Patel, Y. Xu, L. Meshi, J. Dai, Y. Chen, A. Lu, A. V. Davydov and L. Hu, *ACS Appl. Mater. Interfaces*, 2016, **8**, 11390–11395.
2. C. Peng, H. Lyu, L. Wu, T. Xiong, F. Xiong, Z. Liu, Q. An and L. Mai. *ACS Appl. Mater. Interfaces*, 2018, **10**, 36988–36995.
3. Y. Luo, J. Han, Q. Ma, R. Zhan, Y. Zhang, Q. Xu and M. Xu, *ChemistrySelect*, 2018, **3**, 9807–9811.
4. B. Xu, X. Ma, J. Tian, F. Zhao, Y. Liu, B. Wang, H. Yang and Y. Xia, *Ionics*, 2019, **25**, 4171–4177.
5. Y. Subramanian, G. K. Veerasubramani, M. S. Park and D. W. Kim, *J. Electrochem. Soc.*, 2019, **166**, A598-A604.
6. M. Chen, L. Wang, X. Sheng, T. Wang, J. Zhou, S. Li, X. Shen, M. Zhang, Q. Zhang, X. Yu, J. Zhu and B. Lu, *Adv. Funct. Mater.*, 2020, **30**, 2004247.

7. Q. H. Nguyen, H. Kim, T. Kim, W. Choi, J. Hur, *Chem. Eng. J.*, 2020, **382**, 122981.
8. X. Wu, B. Wu, H. Wang, Q. Zhuang, Z. Xiong, H. Yi, P. Xu, G. Shi, Y. Guo and B. Wang, *Energy Fuels*, 2021, **35**, 11563–11571.
9. Q. Peng, F. Ling, H. Yang, P. Duan, R. Xu, Q. Wang and Y. Yu, *Energy Storage Mater.* 2021, **39**, 265–270.
10. L. F. Zhou, X. W. Gao, T. Du, H. Gong, L. Y. Liu and W. B. Luo, *Chem. Eng. J.*, 2022, **435**, 134838.